Oligomer Assembly of the C-Terminal DISC1 Domain (640-854) Is Controlled by Self-Association Motifs and Disease-Associated Polymorphism S704C

ARTICLE *in* BIOCHEMISTRY · AUGUST 2009

Impact Factor: 3.02 · DOI: 10.1021/bi900901e · Source: PubMed

12 AUTHORS, INCLUDING:

Max Michel
Max Planck Institute of Biophysics
5 PUBLICATIONS **66** CITATIONS
SEE PROFILE

Verian Bader
Heinrich-Heine-Universität Düsseldorf
20 PUBLICATIONS **431** CITATIONS
SEE PROFILE

Carsten Korth
Heinrich-Heine-Universität Düsseldorf
116 PUBLICATIONS **2,855** CITATIONS
SEE PROFILE

7746 *Biochemistry* **2009,** *48,* 7746–7755
DOI: 10.1021/bi900901e

BIOCHEMISTRY
including biophysical chemistry & molecular biology
Article

Oligomer Assembly of the C-Terminal DISC1 Domain (640−854) Is Controlled by Self-Association Motifs and Disease-Associated Polymorphism S704C[†]

S. Rutger Leliveld,[‡,§,⊥] Philipp Hendriks,[‡,⊥] Max Michel,[‡,⊥] Gustavo Sajnani,[∥] Verian Bader,[‡] Svenja Trossbach,[‡] Ingrid Prikulis,[‡] Rudolf Hartmann,[§] Esther Jonas,[§] Dieter Willbold,[§] Jesús R. Requena,[∥] and Carsten Korth*[,‡]

[‡]*Department of Neuropathology, Heinrich-Heine University Dusseldorf, 40225 Dusseldorf, Germany,* [§]*Institute for Structural Biochemistry (ISB-3), Research Centre Julich, 52425 Julich, Germany, and* [∥]*Department of Medicine, University of Santiago de Compostela, 15782 Santiago de Compostela, Spain* [⊥] *These authors contributed equally*

Received May 27, 2009; Revised Manuscript Received July 5, 2009

ABSTRACT: Genetic studies have established a role of disrupted-in-schizophrenia-1 (DISC1) in chronic mental diseases (CMD). Limited experimental data are available on the domain structure of the DISC1 protein although multiple interaction partners are known including a self-association domain within the middle part of DISC1 (residues 403−504). The DISC1 C-terminal domain is deleted in the original Scottish pedigree where DISC1 harbors two coiled-coil domains and disease-associated polymorphisms at 607 and 704, as well as the important nuclear distribution element-like 1 (NDEL1) binding site at residues 802−839. Here, we performed mutagenesis studies of the C-terminal domain of the DISC1 protein (residues 640−854) and analyzed the expressed constructs by biochemical and biophysical methods. We identified novel DISC1 self-association motifs and the necessity of their concerted action for orderly assembly: the region 765−854 comprising a coiled-coil domain is a dimerization domain and the region 668−747 an oligomerization domain; dimerization was found to be a prerequisite for orderly assembly of oligomers. Consistent with this, disease-associated polymorphism C704 displayed a slightly higher oligomerization propensity. The heterogeneity of DISC1 multimers in vitro was confirmed with a monoclonal antibody binding exclusively to HMW multimers. We also identified C-terminal DISC1 fragments in human brains, suggesting that C-terminal fragments could carry out DISC1-dependent functions. When the DISC1 C-terminal domain was transiently expressed in cells, it assembled into a range of soluble and insoluble multimers with distinct fractions selectively binding NDEL1, indicating functionality. Our results suggest that assembly of the C-terminal domain is controlled by distinct domains including the disease-associated polymorphism 704 and is functional *in vivo*.

The search for a specific molecular basis of chronic mental diseaes (CMD), such as schizophrenia or affective disorders, has been gaining momentum over the past decade. Among the candidate genes that have been identified so far, disrupted-in-schizophrenia-1 (DISC1)[1] is widely considered as one of the most promising targets (*1*, *2*). The DISC1 gene was positionally cloned following a long-term study of a Scottish family with a high prevalence of psychiatric disease with mixed phenotypes (*3*, *4*). Mutation-bearing family members were found to carry a partial DISC1 gene deletion due to a balanced translocation between chromosomes 1 and 11 (*4*, *5*). As a consequence, the DISC1 gene consisting of thirteen exons is abrogated between exons 8 and 9, corresponding to a C-terminally truncated DISC1 protein with 597 instead of 854 residues (*4*).

Cell biological (*6*) and genetic studies in transgenic mouse lines that express truncated DISC1 corresponding to the human mutation (*7*−*9*) have shown clear cellular and behavioral phenotypes that are consistent with a dominant negative effect of mutant DISC1. So far, such a shortened DISC1 gene product has not been detected in lymphocytes of the familial patients (*10*), although that does not exclude its existence in other tissues, including the brain. As long as the expression of a truncated DISC1 protein in human deletion carriers with CMDs has not been demonstrated, the disease mechanism might therefore also hinge on haploinsufficiency of DISC1 (*2*). These two models of a disease mechanism are not mutually exclusive.

In addition to the Scottish pedigree with familial CMD, several groups have reported an association of single nucleotide polymorphisms within the DISC1 locus with CMD (*11*−*13*). Findings on the exonic polymorphism at residue 704 have not been unequivocal so far: while serine at residue 704 (S704) was reported to be associated with schizophrenia in one study (*14*), other studies implicated cysteine at residue 704 (C704) in major depression, a reduction of the amount of gray matter in the

[†]Funded by a research grant (LE 2197/1-1) to S.R.L. from the German Research Foundation (DFG) and Stanley Medical Research Institute, Baltimore, MD, to C.K.

*Address correspondence to this author: tel, +49-211-8116153; fax, +49-211-8117804; e-mail, ckorth@uni-duesseldorf.de.

[1]Abbrevations: DISC1, disrupted-in-schizophrenia-1 protein; NDEL1, nuclear distribution element-like 1 protein; CCD, coiled-coil domain; mAB, monoclonal antibody; r, recombinant; MW, molecular weight; SEC, size exclusion chromatography; ESI-MS, electrospray ionization mass spectrometry; MALDI, matrix-assisted desorption ionization; CD, circular dichroism; NMR, nuclear magnetic resonance; β-ME, β-mercaptoethanol; HSQC, heteronuclear single-quantum coherence spectra; R_H, hydrodynamic diameter; DLS, dynamic light scattering; IMAC, immobilized metal affinity chromatography; CHAPS, 3-((3-cholamidopropyl)dimethylammonio)-1-propanesulfonate; RPC, reversed-phase chromatography.

 Published on Web 07/07/2009

cingular cortex (*15*), schizophrenia (*16*), or cognitive decline during normal aging (*17*). The broad range of DISC1-assciated phenotypes suggests that the neurophysiological role of DISC1 touches upon CMD in general and not just schizophrenia.

In humans, DISC1 is most abundantly expressed in brain, heart, and placenta (*4*). It is found in the cytoplasm, nucleus, at the centrosome and is associated with mitochondria. DISC1 interacts with a steadily growing list of proteins such as PDE4B, FEZ1, LIS1, nuclear distribution element-like protein 1 (NDEL1), GSK3β, and several cytoskeletal components (*10*, *18*−*23*). Here, NDEL1 is among the most well established binding partners of DISC1 (*6*, *24*). DISC1 is commonly pictured as a central pillar of an extensive protein−protein "interactome" that regulates many aspects of neuronal development and functioning (*6*, *25*−*27*).

At present, a role of nonmutant DISC1 in sporadic cases of CMD in only emerging. Posttranslational modifications in DISC1 are one possibility of how nonmutant DISC1 protein can become dysfunctional. We previously demonstrated DISC1 insolubility as a phenotype in a subset of sporadic cases with CMD (*28*). The critical binding of DISC1 to NDEL1 could be modeled by bacterially expressed C-terminal DISC1 fragments (rDISC598, residues 598−854), showing that only rDISC598 octamers but not the dimers or high molecular weight (MW) multimers bound to NDEL1 (*28*). We concluded that self-association of the DISC1 C-terminus and presumably of DISC1 as a whole was critical for its molecular interactions and thereby for DISC1-related mental and behavioral phenotypes.

According to a consensus prediction of secondary structure, DISC1 is predominantly α-helical, whereby the N-terminus up to residue ~320 is mostly nonstructured (*29*−*31*). The most obvious features in the sequence upward of residue 320 are four putative coiled-coil domains (CCDs) that are situated between residues 400 and 830 (Figure 1A). CCDs are well-characterized and ubiquitous protein−protein interaction motifs (*32*), and DISC1-CCD between residues 462 and 496, for example, features five consecutive matches for the "classical" CCD heptad motif (*33*); a section of DISC1 (residues 403−504) has indeed been shown to be a functional self-association domain (*6*). Two of the four predicted CCDs are located in the C-terminus that is deleted in familial CMD (Figure 1A).

Our motivation for further studies on the C-terminus was based on the following issues: (1) clustering of disease-associated exonic polymorphisms (F/L607 and S/C704) suggesting a functional significance, (2) our previous studies suggesting novel dimerization and/or oligomerization motifs within DISC1, and (3) the possibility whether C-terminal fragments could arise as degradation products *in vivo* and, if so, whether they would be functional.

To clarify the role of the predicted CCDs in this behavior, we report here on self-association and assembly of the DISC1 C-terminus and of several additional truncated fragments (see Figure 1B). We identified a novel dimerization motif roughly coinciding with the last CCD and an oligomerization domain within residues 668−747 of DISC1. Disease-associated polymorphism C704 led to a slightly higher oligomerization. DISC1 C-terminally fragments were identified in human brains and corresponding fragments when transiently expressed in cells bound to NDEL1 indicating functionality.

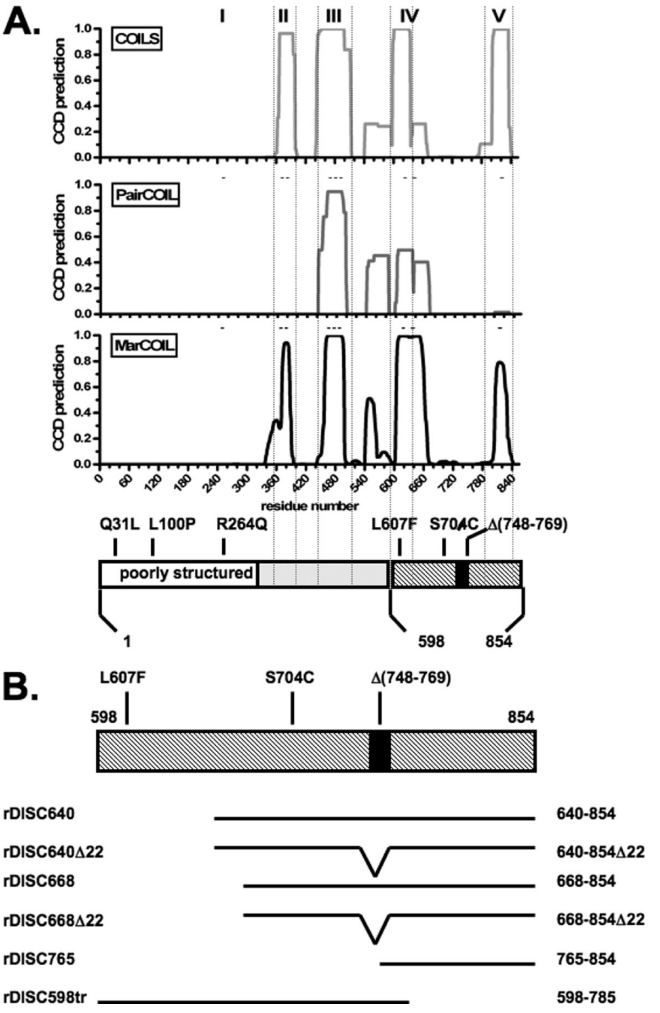

FIGURE 1: Schematic presentation of the DISC1 structure and C-terminal constructs. (A) Location of predicted coiled-coil domains (CCD) in full-length human DISC1, showing the per-residue predictions (28-residue window, MTIDK matrix) of three different CCD-scoring methods: COILS (with weighting) (*44*), Paircoil2 (*45*), and Marcoil (*46*). At the bottom, a bar representation of the DISC1 sequence is shown featuring the variants of the C-terminal domain published so far. Polymorphisms (R264Q, L607F, S704C), the splice variant with a 22-residue deletion (748−769), or artificial mutations (Q31L, L100P) are indicated on top of the bar. Vertical gridlines are shown to facilitate CCD mapping on the structural features. (B) Nomenclature and schematic view of the different recombinant, C-terminal DISC1 fragments used to map self-association domains. Abbrevations of constructs are indicated on the left.

EXPERIMENTAL PROCEDURES

Materials. Buffer components were from Carl Roth GmbH (Germany) or Sigma-Aldrich (USA), antibiotics from Duchefa (The Netherlands), and enzymes from Fermentas (Germany) except for thrombin (Roche, Switzerland). Purification media were from Amersham Biosciences (United Kingdom) except for Ni^{2+}-NTA agarose (Qiagen, Germany). Standard antibodies used included 9E10 α-Myc mAB (Developmental Hybridoma Bank, USA), α-His mAB (Qiagen, Germany), or peroxidase-conjugated α-GST goat polyclonal (Novus Biologicals, USA). BA8 frozen cortex tissue from the Consortium Collection was obtained from the Stanley Medical Research Institute, Baltimore, MD (*34*). These brains were from two cases with schizophrenia, two cases with bipolar disorder, one case with depression, and two normal controls. No genotyping of DISC1 had been performed on these brains.

Cloning of Expression Vectors. (*A*) *Full-Length DISC1*. The open reading frame (ORF; Gln264/Leu607/Ser704 variant) of full-length human DISC1(1−854) was amplified by PCR from

pRK5-DISC1 (gift from Akira Sawa) and inserted into pET-16b (Novagen, USA) at *Nde*I/*Bam*HI (N-terminal decahistidine tag) and into a modified pET-22b vector at *Nde*I/*Eag*I (C-terminal MycHis$_6$ tag, PAEEQKLISEEDLEH$_6$). We subsequently cloned the DISC1(1−854)-MycHis$_6$ ORF into pGEX-4T-3 (Amersham) at *Eco*RI/*Sal*I, which expresses rDISC1 as an N-terminal GST fusion protein. Expression in human neuroblastoma (NLF) cells was performed with pRK5-DISC1 S704 (gift of Akira Sawa) or constructs that had been mutated by QuickChange (Stratagene) to DISC1 C704 or DISC1 S704Δ22; transfection and expression haves been described (*28*). DISC1-(640−854) constructs were also cloned into pcDNA3.1.

(*B*) *C-Terminal DISC1 Fragments*. The DISC1(640−854, 668−854, 598−785) ORF was inserted into pET-15b and pET-22b vectors at *Bam*HI/*Sal*I and *Nde*I/*Eag*I, respectively. Here, pET-15b has been modified to add an N-terminal hexahistidine tag plus thrombin cleavage site (MGSS-H$_6$-SSGLVPRGS). The DISC1(765−854) ORF was cloned into pET-15b and pGEX-4T-3 at *Bam*HI/*Sal*I and *Bam*HI/*Eco*RI, respectively. As a control for NDEL1 binding, we also cloned DISC1(598−854) into pGEX-4T-3 at *Bam*HI/*Sal*I (*24*).

(*C*) *NDEL1*. The human NDEL1(1−345) ORF was amplified from pcDNA-NDEL1 (gift from Li-Huei Tsai) and cloned as described for DISC1(765−854).

Expression and Purification. (*A*) *Culture and Lysis*. All rDISC1 constructs were expressed in *Escherichia coli* BL21-(lDE3) Rosetta (Novagen) at 37 °C in Luria−Bertoni medium (plus 5 mM L-arginine, 5 mM $MgSO_4$, 100 μg/mL carbenicillin, and 35 μg/mL chloramphenicol). Expression was induced at midlog phase with 1 mM isopropyl β-D-1-thiogalactopyranoside (IPTG) for 3 h. GST-DISC1(765−854) was additionally expressed in minimal medium (M9 salts, 0.4% glucose, 1 g/L $^{15}NH_4Cl$ plus vitamins, trace elements, and antibiotics). Both rNDEL1 constructs were expressed at 25 °C for 4 h. Cells were lysed in 50 mM Tris-HCl, pH 8, 5 mM EDTA, 1% Triton X-100, 2 mM phenylmethanesulfonyl fluoride (PMSF), 20 mM β-mercaptoethanol (β-MeOH), and 0.25 mg/mL lysozyme, followed by DNase I treatment (plus 20 mM $MgCl_2$). After addition of 500 mM NaCl and 5 mM imidazole, the soluble fraction was collected by centrifugation (20 min at 15000*g*). The remaining pellet was solubilized in 50 mM Tris-HCl, pH 8, 2 mM imidazole, 500 mM NaCl, 20 mM β-MeOH, and 6 M guanidine hydrochloride (GnHCl; overnight, 4 °C).

(*B*) *Nondenaturing Purification*. His-tagged proteins were purified using Ni^{2+}-NTA agarose:immobilized metal-affinity chromatography (IMAC). The column was washed with 20 mM Tris-HCl, pH 8, 10 mM imidazole, 500 mM NaCl, and 1% 3-((3-cholamidopropyl)dimethylammonio)-1-propanesulfonate (CHAPS), followed by buffer plus 50 mM imidazole (35 mM for His$_6$-NDEL1) without detergent. Protein was eluted with 200 mM imidazole, then supplemented with 1 mM phenylmethanesulfonyl fluoride (PMSF), and dialyzed to TBSE (10 mM Tris, pH 8, 150 mM NaCl, 1 mM EDTA). Lysate containing GST-tagged protein was applied to GSH-Sepharose and then washed with 20 mM Tris-HCl, pH 8, 500 mM NaCl, 1 mM EDTA, 20 mM β-ME, and 1% CHAPS. Protein was eluted with 50 mM Tris-HCl, pH 8, 1 mM EDTA, and 20 mM reduced glutathione (GSH) and then dialyzed as above.

(*C*) *Denaturing Purification*. Guanidine hydrochloride (GnHCl) solubilized His$_{10}$-DISC(1−854) was combined with IMAC beads and stirred overnight, supplemented with 10 mM $MgCl_2$ to block traces of EDTA. Beads were washed with GnHCl extraction buffer plus 10 mM imidazole and then eluted with the same buffer with 150 mM imidazole. His$_{10}$-DISC1(1−854) was concentrated to 5 mg/mL and supplemented with 1% β-MeOH and 2 mM EDTA. For His$_6$-DISC640, the GnHCl extract was directly applied to a Ni^{2+}-NTA agarose column and washed as above. Bound protein was refolded in one step by washing with 20 mM Tris, pH 8, 10 mM imidazole, 20 mM β-MeOH, and 500 mM NaCl (∼30 min, 4 °C), followed by elution as described.

(*D*) *Preparative Size Exclusion Chromatography* (*SEC*). We fractionated IMAC-purified rDISC(1−854)-MycHis$_6$ and on-column refolded His$_{10}$-DISC1(1−854) (see above) on a Sephacryl S-300 HR 26/60 in TBSE, 0.5% *N*-lauroylsarcosine (sarkosyl), and 10 mM β-MeOH at room temperature, using a BioLogic LP system (Bio-Rad, USA). For preparative purposes, we separated rDISC598, rDISC640, and rDISC765 in a low-MW (dimer, < 75 kDa) and a high-MW (oligomers plus multimers) fraction on a HiLoad 26/60 Sephacryl 75 column in TBSE plus 10 mM β-ME (at 4 °C) using an Akta-FPLC (Amersham).

(*E*) *Reversed-Phase Chromatography*. To isolate the ∼27 kDa C-terminal fragment of rDISC(1−854)-MycHis$_6$, we fractionated the IMAC eluate (see Figure 1) by reversed-phase chromatography (RPC) on a Resource RPC3 column using a 0−60% 2-propanol gradient (90 min, 0.5 mL/min) in 25 mM NH_4HCO_3, pH 9, at room temperature. Both the fragment and rDISC640-MycHis$_6$ eluted at 35% 2-propanol.

(*F*) *Thrombin Cleavage*. rDISC1 (1−3 mg/mL, 20 mM Tris-HCl, pH 8.3, 300 mM NaCl, 1 mM EDTA) was digested with thrombin (0.1 unit/mg for His$_6$-DISC640, 0.4 unit/mg for GST-DISC765) at room temperature for up to 2 h. Digest was stopped by adding 2 mM PMSF. Cleaved ^{15}N-GST-DISC765 was passed twice over fresh GSH-Sepharose, followed by removal of noncleaved GST-DISC765 by SEC.

Biochemical and Biophysical Analysis. (*A*) *Analytical SEC*. Oligomer size distribution was determined using an Akta-HPLC system (Amersham) equipped with a Superdex S200 10/300 GL column (200 mL sample, 0.5 mL/min TBSE plus 10 mM β-ME). The column was calibrated using gel filtration molecular weight markers (MW-GF-1000; Sigma).

(*B*) *CD Spectroscopy*. Spectra were recorded on a Jasco J-815, using either a 0.2 cm (far-UV, 1−5 μM protein) or a 1.0 cm (near-UV, 100 μM protein) cuvette. Settings: 1 nm bandwidth, 50 nm/min scan, 2 s response time, 40 accumulations. Buffer: 10 mM $NaPO_4$, pH 8, and 0.1 mM EDTA at 20 °C. Spectra were normalized to molar ellipticity units ([θ] in 10^3 deg cm^2 dmol^{-1}) per residue. CDSSTR secondary structure estimates were performed at DICHROWEB (*35*). In each case, the normalized root-mean-square deviation (NRMSD) between experimental data and fitted curve was ≤0.01.

(*C*) *Dynamic Light Scattering*. Protein scattering profiles were recorded in a 3 mm cuvette on a DynaPro MS/X with temperature controller (Wyatt Technology, USA) in TBSE and 10 mM β-ME. Data were analyzed by DYNAMICS V6. All R_H values are averages (±SEM) based on at least four separate data sets of ten measurements each.

(*D*) *rNDEL1 Binding*. His$_6$-DISC640 and rDISC640-MycHis$_6$ were first fractionated into dimers and oligomers/multimers in assay buffer (20 mM Tris-HCl, pH 8, 10 mM imidazole, 500 mM NaCl, 10 mM β-ME, 0.5% CHAPS) and then directly loaded onto Ni^{2+}-NTA agarose beads. These were subsequently incubated (30 min, room temperature) with SEC-purified GST-NDEL1 at a roughly equimolar monomer ratio. Beads were washed and then eluted with TBS and 50 mM EDTA. Pulldown

of His_6-NDEL1 with GST-DISC765 and GST-DISC598 was performed under comparable conditions, using GSH-Sepharose. Samples were Western blotted and detected with the appropriate antibody. For analysis of oligomer-specific binding, rDISC640 was labeled cysteine-selectively with fluorescein-5-maleimide (Invitrogen, USA), combined with nonlabeled His_6-NDEL1 (1:4 molar monomer ratio), and fractionated by analytical SEC (monitored at 495 nm).

(*E*) *Cell Transfections and Assays*. Human neuroblastoma cells (NLF; Children's Hospital of Philadelphia, Philadelphia, PA) were grown to 70% confluency in 60 mm plates and transfected with 8 μg of pcDNA-DISC1 plasmid using Metafectene reagent (Biontex, Martinsried, Germany). After 24 h cells were lyzed and subjected to a DNA digest for 30 min in 300 μL of lysis buffer (50 mM HEPES, pH 7.5, 300 mM NaCl, 250 mM sucrose, 10 mM $MgCl_2$, 1% NP-40, 0.2% sarcosyl, 2× PI (Roche), 1 mM PMSF, and DNase I, 40 units/mL) and incubated at 4 °C overnight. Samples were then centrifuged for 30 min at 1800*g* and resuspended in high salt buffer (50 mM HEPES, pH 7.5, 1.5 M NaCl, 250 mM sucrose, 1% NP-40, 0.2% sarcosyl, 2× PI (Roche), 1 mM PMSF). Subsequently, samples were centrifuged for 30 min at 1800*g*, and the resulting pellet was resuspended in 300 μL of cold 50 mM HEPES and 0.2% sarcosyl. Finally, probes underwent ultracentrifugation at 100000*g* for 45 min at 4 °C (TLA-55 rotor in Optima; Beckman Coulter), and the resulting pellet was solubilized in SDS loading buffer. All steps were performed on ice unless otherwise stated.

(*F*) *Glycerol Gradients*. NLF cells were transfected for 24 h with pcDNA DISC1(640−854 S/C704) prior to washing with ice-cold PBS and immediate lysis in 450 μL of lysis buffer (10 mM HEPES, pH 7.5, 2 mM $MgCl_2$, 10 mM KCl, 0.50% NP-40, 0.5 mM EDTA, 150 mM NaCl, 1 mM DTT, 10 mM PMSF, 1× PI). After 20 min incubation on ice the lysate was pelleted at full speed in a microcentrifuge for 5 min at 4 °C. The supernatant was loaded on top of a glycerol gradient. Glycerol gradients were created by layering 450 μL of gradient solutions (90−10% glycerol in 10 mM HEPES, pH 7.5, 2 mM $MgCl_2$, 10 mM KCl, 0.5 mM EDTA, 150 mM NaCl; all solutions sterile-filtered at 0.45 μm) in 5 mL ultracentrifugation tubes (Beckman Coulter, MLS50 rotor in an Optima ultracentrifuge) for 18 h at 4 °C and 100000*g*. The glycerol fractions were collected from top to bottom, and 200 μL was used immediately for TCA precipitation of the proteins. The protein pellet was resuspended in 2× SDS sample buffer, heated for 5 min at 95 °C, and loaded on a 10% SDS−PAGE gel.

(*G*) *Brain Homogenates*. Human brains were homogenized as a 10% solution in lysis buffer in the presence of protease inhibitors (Roche) and 10 mM PMSF. Immunoreactivity to dihydropyrimidase-related protein 2 (*36*) had previously shown that all used brains had not been subject to spontaneous degradation (*28*).

(*H*) *Native Gels and Western Blotting*. Native PAGE gels (11%, 380 mM Tris-HCl, pH 8.0) with a 3.6% stacker (70 mM Tris-HCl, pH 8.0) were run in 1× Tris−glycine buffer, pH 8.3, at 150 V (4 °C). Protein samples were diluted in Tris−glycine buffer, 10% w/w glycerol, and 0.01% w/v bromphenol blue and loaded at 200 ng per lane for immunoblots and 6 μg for Coomassie-stained gels. After blotting of native PAGE gels onto nitrocellulose (at 4 °C), blots were developed with mABs 19F7, 2C7, and FFD5 antiserum (*28*) at room temperature.

(*I*) *Monoclonal Antibodies*. mABs 19F7, 2C7, 18G6, and 3B12 were generated by standard techniques as described previously in different fusions (*37*). Briefly, mice were immunized and boosted with 100 μg of rDISC1 (598−854; mABs 19F7, 2C7) or KLH-coupled peptides (mAB 18G6, 832AKEAGER-EAAASCMT846; mAB 3B12, 665KENTMKYMET674) suspended in RIBI adjuvant (Sigma), three times at 3 week intervals; a final intraperitoneal boost was done 1 and 2 days before fusion of splenocytes with myeloma cells. Hybridoma supernatants were then screened for recognition of a mix of all rDISC598 species on enzyme-linked immunofiltration assay (ELIFA) as described (for mAB 19F7; ref *37*) or on ELISA against the immunogen (mABs 2C7, 18G6, 3B12). For Western blotting, antibodies were used as diluted hybridoma supernatants.

(*J*) *Statistics*. To compare oligomer propensity of rDISC640 S704 vs C704, areas under the curve from elution time 10 min to the lowest point between the oligomer and dimer peaks were measured (NIH ImageJ), normalized, and compared by Student's *t* test. For comparing different efficiencies of the pulldown of DISC1-transfected cell lysates by recombinant GST-NDEL1, densitometric measurements (NIH ImageJ) of four independent experiments were normalized, averaged, and compared by Student's *t* test.

RESULTS

Selection and Expression of C-Terminal Fragments. To investigate the oligomerization propensity and motifs of C-terminal DISC1, we cloned a series of constructs including or excluding the third or fourth CCD, as well as constructs identified as stable, distinct C-terminal degradation products of full-length DISC1 (Figure 1B).

During expression of full-length rDISC1(1−854)-$MycHis_6$ in *E. coli*, we noticed that a set of spontaneously arising C-terminal fragments, ranging in size from 15 to 27 kDa, as suggested by SDS−PAGE, were soluble under nondenaturing conditions (Supporting Information Figure 1). Mass spectrometry analysis (ESI-MS) showed that the MW of the most abundant fragment of rDISC1 (1−854) was 23447.1 Da, suggesting a cleavage site at or near residue 668 (Supporting Information Figure 2). The smallest species we detected had a MW of 13372.3 Da, corresponding to residues 756−854. We therefore expressed and tested the following four truncation constructs (see also Figure 1B): (1) residues 668−854 (rDISC668), (2) residues 640−854 (rDISC640), (3) residues 765−854 (rDISC765), and (4) residues 598−785 (rDISC598tr). In addition, we cloned rDISC598tr, rDISC668, and rDISC640 as S704 and C704 variants. For rDISC640 and rDISC668, we also cloned each variant with the splice variant termed Δ22, in which residues 748−769 are deleted. These residues have been shown to be relevant required for NDEL1 binding (*27*, *38*).

We included rDISC640 since it mimics the largest C-terminal fragment (27 kDa) seen on Western blot and because its N-terminal truncation site at G640 lies in a predicted hinge region. Likewise, rDISC765 represents the smallest fragment after cleavage at the predicted hinge region near G765. Both rDISC668 and rDISC765 contain only the fourth and last predicted CCD (residues 802−830), while rDISC598tr contains only the third CCD (residues 599−670).

The Fourth Predicted CCD in DISC1 Leads to Formation of Dimers. Similar to our previous observations with rDISC598 (*28*), both rDISC668 and rDISC640 formed a mixture of dimers, one or two types of oligomer, and soluble multimers (> 400 kDa), as shown by SEC (Figure 2A,B) and covalent cross-linking (Supporting Information Figure 3A). Although the dimer

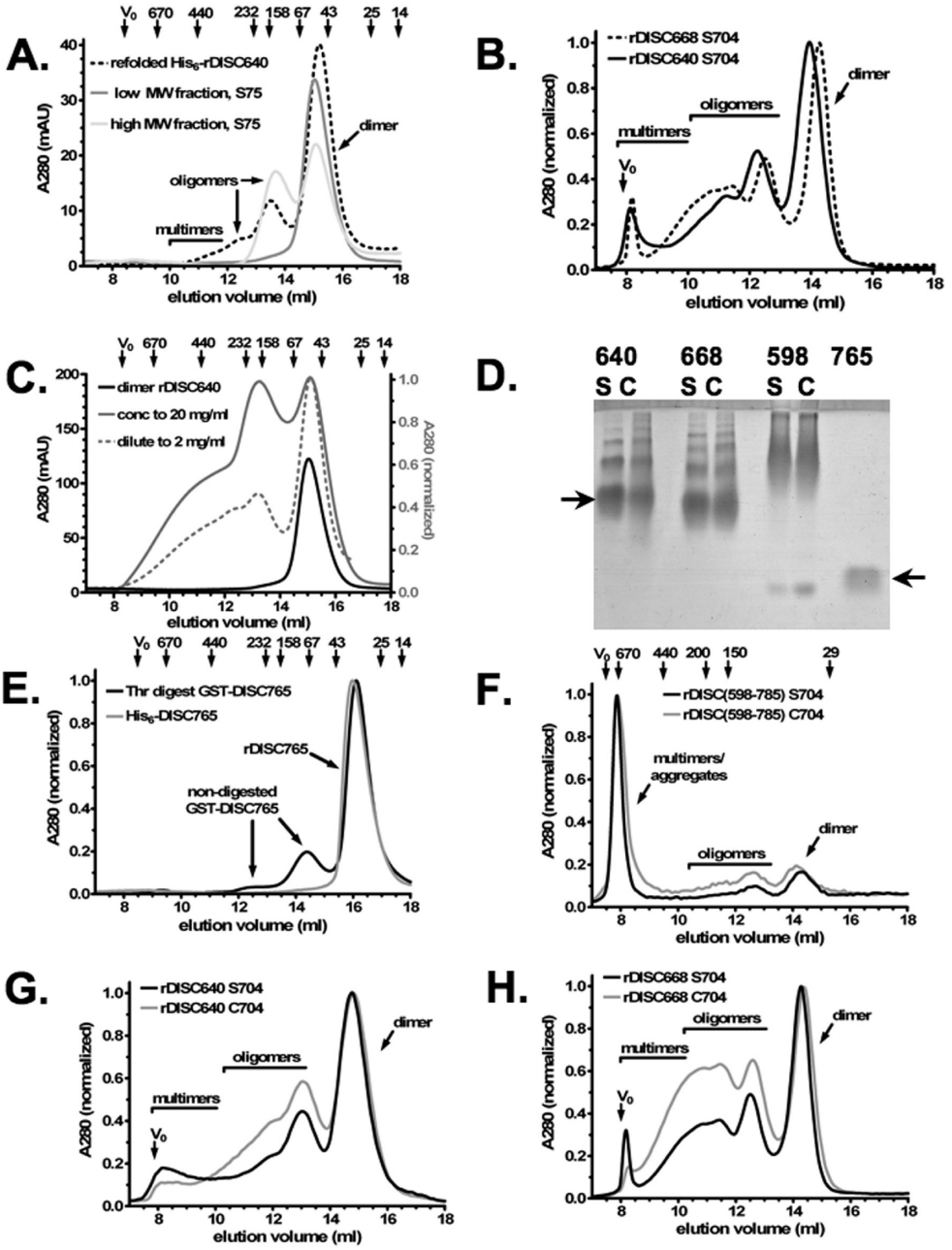

FIGURE 2: Oligomerization of C-terminal DISC1 fragments. (A) SEC profile of refolded His_6-DISC640 (S704) before (dashed line) and directly after preparative separation into a low-MW (below 75 kDa) and high-MW (above 75 kDa) fraction, showing an asymmetric equilibrium: part of the isolated oligomers (light gray) rapidly dissociate to dimers while isolated dimers do not associate into oligomers at the same speed (dark gray). (B) Comparison of SEC of rDISC(640−854) and rDISC(668−854), both S704, showing that the truncation site has only minor effects on the size distribution. (C) Profile of isolated rDISC640 dimers before (black line) and after concentration to 20 mg/mL (0.75 mM, gray line), followed by a 10-fold dilution (dashed line). The large shifts in size distribution illustrate that rDISC640 oligomerizes reversibly in a concentration-dependent manner. (D) Native Coomassie PAGE of bacterially expressed rDISC1 640−854 ("640"), DISC1 668−854 ("668"), DISC1 598−785 ("598"), and DISC1 765−854 ("765"), with serine ("S") or cysteine ("C") at codon 704. The arrow demarks the electrophoretic mobility of the rDISC640 dimer (left) or rDISC765 dimer (right). (E) Profile of rDISC765 as the His_6-tagged construct and after cleavage from GST-DISC765: both elute exclusively as dimers (~30 kDa). A fraction of intact GST-DISC765 is still present, eluting mainly as a dimer of ~70 kDa. Larger complexes form due to the dimerizing tendency of GST itself. (F) Comparison of rDISC(598−785)-S704 (black line) versus rDISC(598−785)-C704 (gray line), showing that loss of the C-terminal CCD disrupts ordered oligomerization of the DISC1 C-terminal fragment. (G) SEC profile of rDISC640-S704 (black line) versus rDISC640-C704 (gray line), showing that both have the same basic size distribution but that the C704 variant has a moderately higher tendency toward oligomerization. (H) Comparison of rDISC668-S704 (black line) versus rDISC668-C704 (gray line), showing higher oligomer content for the C704 variant.

could be isolated as a stable species, part of the oligomers would immediately dissociate to dimers after fractionation (Figure 2A). This behavior was illustrated by DLS: the rDISC640 dimer had an R_H of 3.1 ± 0.4 nm (45 ± 15 kDa), and the oligomer plus multimer fraction had an R_H of 3.9 ± 0.2 nm (80 ± 10 kDa), just like the nonfractionated sample. CD spectroscopy of the rDISC640 dimer fraction and the combined oligomer/multimer fraction directly after SEC showed that both contained the same overall folding, namely, mixed α/β (Supporting Information Figure 4). Unlike rDISC598, rDISC640 did not have an aggregation threshold; instead, its size distribution shifted toward oligomers and dimers upon concentration (Figure 2C).

SEC showed that rDISC765 only formed a ~35 kDa species (Figure 2E). Covalent cross-linking showed this presumably nonglobular complex to be dimeric (Supporting Information Figure 3B). Because of recurring protease contamination in the His-tagged construct (data not shown), we carried out SEC using rDISC765 cleaved from GST-DISC765. CD spectroscopy showed rDISC765 to be mainly α-helical, which is consistent with the presence of a CCD (Supporting Information Figure 4). The 2D NMR spectrum of ^{15}N-labeled rDISC765 (pH 4) did not allow for further structure elucidation, showing relatively poor dispersion of amide chemical shifts, irrespective of buffer conditions (Supporting Information Figure 4C).

The Third Predicted CCD in DISC1 Leads to Formation of Multimers. SEC analysis of rDISC598tr showed mainly high-MW multimers and small amounts of dimers and oligomers (Figure 2F). Its CD spectrum was nevertheless comparable to that of rDISC668 and rDISC640, meaning that overall folding was not affected by truncation (Supporting Information Figure 4A). The predominance of multimers in DISC598tr was corroborated by native PAGE (Figure 2D) and native agarose gel electrophoresis (Supporting Information Figure 5). Here, laddering of DISC1 640−854 and DISC1 668−854 indicated regular oligomerization that was higher and less regular for DISC1 598−785 and absent for DISC1 765−854. No clear differences in S704 vs C704 constructs were discernible. These findings suggested that dimerization encoded by the last CCD was necessary for an orderly, concerted oligomerization together with 668−747.

Influence of the S704/C704 Polymorphism on Oligomerization Behavior of rDISC640. Since the disease-associated exonic polymorphism at residue 704 is located within the oligomerization region, we investigated whether recombinant DISC1 C-terminal fragments expressing either S or C at position 704 would differ in their oligomerization behavior. rDISC640-C704 had, on average, a moderately higher fraction of oligomers than rDISC640-S704 (rDISC640-S704 was 75 ± 15% of rDISC-640-C704; $p = 0.04$), as shown for three separate batches of simultaneous preparations (Figure 2G; Supporting Information Figure 6A). We obtained similar results for rDISC668 (Figure 2H). Furthermore, both rDISC640Δ22-S704 and -C704 constructs, lacking residues 748−769, still had a size distribution like rDISC640 with a higher oligomerization for C704 (Supporting Information Figure 6B). CD spectroscopy of rDISC640 S704 and C704 yielded exactly the same results (Supporting Information Figure 4A).

Taken together, these results indicate that the fourth CCD forms a stable dimer and that the region between residues 668 and 747 is responsible for oligomerization. Although the third CCD is capable of aiding the formation of higher order oligomers and multimers, it is dispensable for oligomerization of the whole C-terminal domain. We conclude that the oligomerization domain, if indeed folded like a CCD, is more likely to be involved homomeric in intramolecular interactions and that the S704C polymorphism that is located in that domain modulates it.

Monoclonal Antibody 19F7 Specifically Recognizes High Molecular Weight Multimers of rDISC640. From mice immunized with a heterogeneous mix of dimers and oligomers of rDISC598 (S704), we isolated a mAB, termed 19F7, that recognized rDISC640 high molecular weight multimers much better than dimers under nondenaturing conditions (Figure 3). This antibody was used to compare rDISC640-S704 to -C704 on native Western blots, i.e., nondenaturing (reducing) PAGE gels that were blotted onto nitrocellulose. Both

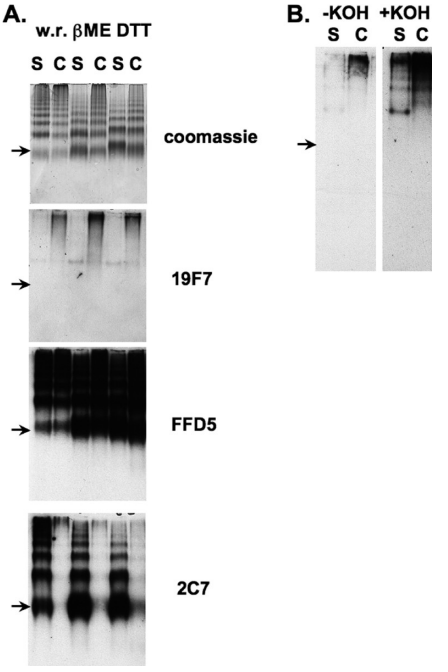

FIGURE 3: Characterization of DISC640 oligomers with a high molecular weight multimer-specific mAB. (A) Multimerization of rDISC640 under nondenaturing conditions as shown by native PAGE gel (11%). Top panel: Coomassie-stained gel. Bottom panels (in descending order): Western blot thereof, developed with α-DISC1 mAB 19F7, polyclonal FFD5, and mAB 2C7. Equal amounts of rDISC640-S704 and rDISC640-C704 were loaded either without reduction (w.r.), with 2% β-mercaptoethanol (βME), or with 10 mM DTT (DTT). As a control antiserum, FFD5 stains both variants equally well. The epitope of mAB 2C7 contains residue S704, at least under nondenaturing conditions, since it stained rDISC640-S704 but not rDISC640-C704. Such an effect is ruled out for mAB 19F7, since it too had been raised against rDISC598-S704. (B) Nondenaturing Western blot of rDISC640-S704 and rDISC640-C704, developed with 19F7, with or without KOH denaturation (±KOH) after blotting. The increase of immunoreactivity of 19F7 after KOH denaturation demonstrates that the epitope of 19F7 is conformation-sensitive and, in lower molecular weight oligomers, hidden in the native conformation. The arrow demarks the electrophoretic mobility of the rDISC640 dimer.

constructs migrated as a regularly spaced ladder, presumably reflecting the dimer−oligomer equilibrium seen by SEC, as could be seen by developing the WB with an all DISC1-recognizing antiserum FFD5 (Figure 3A; see also Figure 2D). Adding reductant dissociated some of the slower migrating bands. mAB 19F7 bound readily to the slow-migrating species of rDISC640-C704, but it recognized those of rDISC640-S704 only weakly. However, the occurrence of HMW bands was not exclusive to DISC 640−854 C704 (data not shown) and rather appeared to be specific for HMW multimers themselves, that could represent, for example, misfolded and/or aggregated assemblies. Polymorphism (S704) specific binding was observed for mAB 2C7, a mAB also identified from a fusion of splenocytes of mice immunized with rDISC598, which reacted much weaker with rDISC598-C704 than with rDISC598--S704, indicating that the 704 polymorphism was part of its epitope (Figure 3A).

The binding preference of 19F7 for high-MW multimeric rDISC640 was found to be conformation-dependent, which we showed by denaturing Western blots with 0.1 M KOH prior to blocking and antibody exposure. As a result, the 19F7 epitope appeared clearer in both rDISC640-S704 and -C704, including in faster migrating multimers, suggesting that the 19F7 epitope was

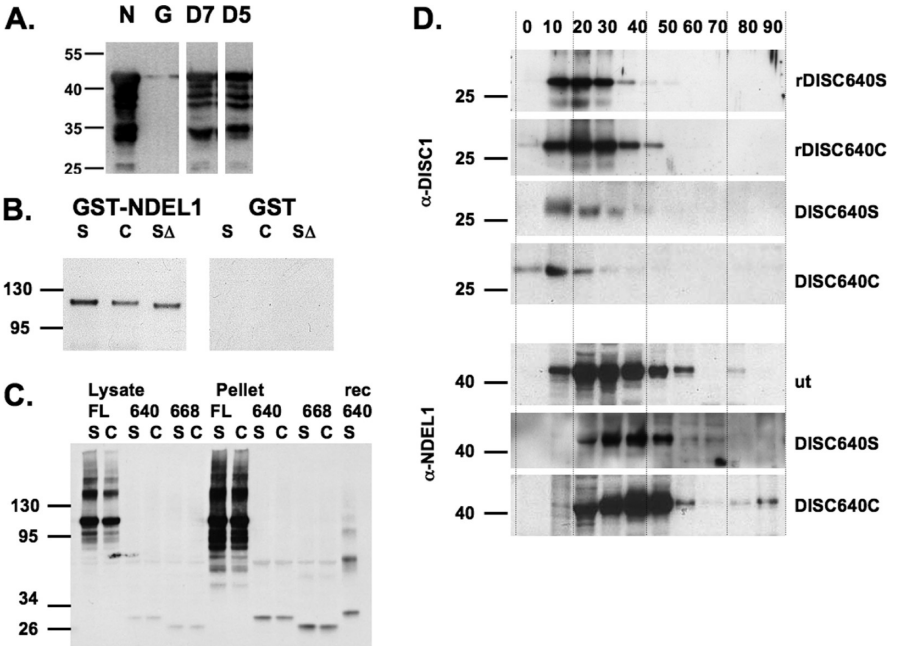

FIGURE 4: Interaction of C-terminal DISC1 with NDEL1. (A) Western blot, developed with α-His mAB, of a pulldown of His_6-rNDEL1 with immobilized GST-DISC765 (D7) or GST-DISC598 (D5). Input material: His_6-NDEL1 (N), pulldown of His_6-NDEL1 with GST (G, negative control), with GST-DISC765 (D7), or with GST-DISC598 (D5). The blot shows that DISC1 765−854 is sufficient to pull down rNDEL1. (B) Western blot, developed with mAB 3D4, of a pulldown of DISC1 expressed in human neuroblastoma cells (NLF) with immobilized GST-NDEL1. Like the bacterially expressed truncated rDISC640 (Supporting Information Figure 7B), GST-NDEL1 pulled down DISC1-S704 ("S"), DISC1-C704 ("C"), and DISC1Δ22-S704 with comparable efficiency. (C) Western blot of lysates or insoluble pellets of human NLF cells transiently transfected with full-length DISC1 ("FL"), DISC1 640−854 ("640"), or DISC1 668−854 ("668"). The blot shows that, similar to full-length DISC1, C-terminal DISC1 has aggregation propensity. (D) Western blots of glycerol gradient fractions (0−90%, as indicated) of bacterially expressed DISC 640−854 S704 (rDISC640S) or DISC 640−854 C704 (rDISC640C), untransfected NLF cells (ut), or transiently transfected NLF cells with DISC 640−854 S704 (DISC640S) or DISC 640−854 C704 (DISC640C). As indicated, the upper four panels were incubated with anti-DISC1 antiserum, and the lower three panels were incubated with anti-NDEL1 antiserum. For DISC640S and DISC640C, the same fractions were incubated with anti-DISC1 (upper panels) and anti-NDEL1 (lower panels) antisera. The blot shows a distribution of DISC640S and DISC640C in the lighter fractions and a shift of the NDEL1 immunoreactivity to heavier fractions upon transient expression of DISC640 without a clear difference in S704 vs C704.

more effectively hidden in rDISC640-S704 than in rDISC640-C704 (Figure 3B). Iodoacetamide treatment of reduced DISC640, to block formation of disulfide bonds by the extra cysteine residue, did not prevent selective staining of high molecular weight rDISC640 by 19F7, indicating that the effects observed were not due to artificial disulfide bond formation (data not shown). Differential immunoreactivity of mAB 19F7 to high-MW rDISC640 is thus another distinction of HMW multimers compared to low-MW oligomers.

Binding of DISC1 640−854 S/C704 Oligomers to NDEL1 in Vitro and in Vivo. To investigate NDEL1 binding of C-terminal DISC1 fragments, we cloned and expressed recombinant NDEL1 in *E. coli*. Correct folding of rNDEL1 was verified by CD spectroscopy (Supporting Information Figure 4). Previously, we had demonstrated that rNDEL1 has a strong preference for binding octameric rDISC598 in solution when a mixture of chromophore-labeled rDISC598 in an excess of nonlabeled rNDEL1 was fractionated (*28*). We performed the same experiment for rDISC640 and again observed how only the oligomers and not the dimers or high-MW multimers were taken up into the ~500 kDa rNDEL1-rDISC1 complex (Supporting Information Figure 7A,B). The shortest DISC1 C-terminal fragment, GST-DISC765, was able to bind bacterially expressed His_6-NDEL1 as effectively as GST-DISC598 (Figure 4A), confirming that the last CCD indeed represents the minimal rNDEL1-binding domain (*24*, *27*). In addition, it showed that the absence of oligomer-forming motifs in rDISC765 did not impair their ability to bind rNDEL1.

Both rDISC640 and rDISC640Δ22 (each with S704 or C704) could be pulled down by GST-NDEL1, with no clear differences in affinity (Supporting Information Figure 7C). A previous paper identified a slightly better pulldown of full-length DISC1-C704 versus DISC1-S704 as well as decreased binding of full-length DISC1Δ22 to NDEL1 when both proteins were coexpressed in mammalian (human embryonic kidney) cells (*27*). GST-NDEL1 also pulled down full-length DISC1-S704 expressed in human neuroblastoma (NLF) cells with decreased binding of DISC1-C704 (87 ± 7% of DISC1-S704; $p = 0.0036$; Figure 4B) or DISC1-S707Δ22 (90 ± 11% of DISC1-S704; $p = 0.16$; Figure 4B). C-Terminal DISC1 expressed as a recombinant protein in NLF cells had an aggregation propensity similar to that of the full-length DISC1 protein (Figure 4C (*28*)). When we analyzed soluble C-terminal DISC1 transiently expressed in NLF cells on a discontinuous glycerol gradient, we observed DISC1 immunoreactivity over several fractions (Figure 4D) with no relevant difference in the size distribution of S704 vs C704 complexes or NDEL1 binding within these complexes. The distribution of DISC1 640−854 over the range of several glycerol fractions showed, however, that this protein interacted with itsself in multimers and/or other proteins and thus was self-associating *in vivo*. For endogenous NDEL1, a shift in the peak expression in the 20% fraction to the 40% fraction upon transient expression of DISC1 640−854 demonstrated that a functional DISC1 interaction was formed and that C-terminal DISC1 fragments were bioactive *in vivo* (Figure 4D). We did not see a dramatic difference of this shift when comparing S704 vs C704, indicating that either the 704 polymorphism effects on

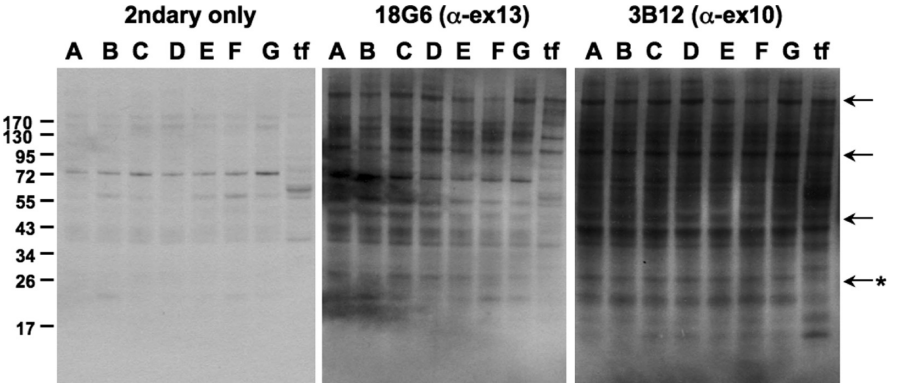

FIGURE 5: Presence of C-terminal DISC1 fragments in human brain. Western blots of human brain homogenates (A−G), incubated with either secondary antibody alone (left panel), mAB 18G6 directed against a peptide from DISC1 exon 13 (middle panel), or mAB 3B12 directed against a peptide from DISC1 exon 10 (right panel). Arrows indicate immunoreactive bands corresponding to DISC1 detected with both mABs but not secondary antibody alone; a star indicates a immunoreactive C-terminal DISC1 fragment. tf = full-length human DISC1 transfected NLF cell lysate control.

NDEL1 binding are subtle or affect mainly interactions with a different protein.

Presence of DISC1 C-Terminal Fragments in Vivo. To investigate whether C-terminal DISC1 fragments occur *in vivo*, we analyzed human brain homogenates for detection of C-terminal fragments with monoclonal antibodies raised against the C-terminus of DISC1 (Figure 5). We detected several distinct imunoreactive bands, one similar in size to a DISC1 C-terminal species (Figure 5, arrow with star). This indicated that C-terminal fragments exist in the adult brain. No association of the presence of C-terminal fragments with disease was noted in this limited collection of samples using mABs 3B12 and 18G6 (Figure 5), as well as in our previous publication using antiserum raised against full-length human DISC1 (*28*). The origin and function of these C-terminal DISC1 fragments are unclear, but they could be the product of a yet undescribed proteolytic pathway.

DISCUSSION

Analysis of the DISC1 protein has lagged behind the elucidation of the role of the DISC1 gene in chronic mental diseases (CMD). Given the established role of posttranslational protein modifications in the disease mechanisms of most degenerative brain conditions (*39*, *40*), there is need for a protein biochemical characterization of the DISC1 protein. The C-terminal DISC1 domain is of key interest since its deletion in the original Scottish pedigree is linked to behavioral phenotypes of CMD. Here, we demonstrate that a C-terminal fragment of rDISC1, roughly corresponding to the domain deleted in the Scottish pedigree with DISC1-associated CMD (*4*), (1) exists *in vivo*, (2) folds into a stable fragment, (3) directs multimerization in an apparently orderly interplay between a dimerization and oligomerization subdomain, and (4) harbors a disease-associated polymorphism that modulates oligomerization. Apart from providing a biochemical phenotype for disease-associated C704, our results suggest that DISC1 C-terminal fragments present *in vivo* may have a yet unappreciated role in modulating DISC1-related cellular functions.

Deciphering structural features of the DISC1 protein is key for determining its role in CMD. Here, we have identified two novel self-association sites within the DISC1 C-terminus: a dimerization site within residues 765 and 854 and an oligomerization site between residues 668 and 748. Our data provide experimental support for the role of CCDs in self-association of the C-terminus, showing that dimerization and higher order oligomerization depend on two different structural units. Our findings extend our previous studies where we identified dimers, octamers, and HMW multimers as possible pathways of assembly of the DISC1 C-terminus (*28*). We show that the CCD presented by residues 598−668 has no role in multimerization, that the last CCD coordinates dimerization, and that a probably unstructured subdomain within residues 668 and 747 controls oligmerization. The dimer−oligomer equilibrium is shifted toward the dimers, since the oligomers build much slower than the oligomers dissociate back to the dimeric subunit (Figure 2C); since the dimer is the state of DISC1 640−854 where NDEL1 is not bound (data not shown; same as in ref *28*), it could be speculated that the fast inactivation of functional oligomer complexes is an efficient way of regulating DISC1 function. With mAB 19F7 we could also present a ligand for HMW aggregates of recombinant DISC1 640−854 as yet more evidence for their distinct conformations (Figure 3). We know that this conformation, similar to the dimers, does not bind NDEL1 (*28*), but we presently do not know whether this HMW multimer arises through simple misfolding or in a more coordinated process.

These data complement those by Kamiya et al. (*6*), who identified a self-association site within DISC1 that was mapped to residues 403−504 of full-length DISC1 by pulldown experiments with deletion mutants expressed in HEK293 cells. The domain 403−504 is overlapping with predicted CCD III (Figure 1A). Further experiments will have to be performed to demonstrate whether these self-association domains in different parts of DISC1 act in concert in the assembly of full-length DISC1 or whether they fulfill different functions. For this paper, it was important to show that the C-terminal domain of DISC1 (640−854) exists *in vivo* (Figure 5), can fold as an independent unit (Supporting Information Figure 4B,C), and uses distinct self-association motifs to orchestrate oligomer assembly (Figure 2E,F).

The analysis of exonic polymorphism at codon 704 in epidemiologic studies has yielded evidence that cysteine at codon 704 is associated with major depression (*15*, *41*), schizophrenia (*16*), or cognitive decline during normal aging (*17*). Residue 704 is located at the oligomerization-coding polypeptide stretch 668−747, and we could show that C-terminal DISC1 C704 fragments do oligomerize slightly higher than S704 (Figure 2G,H). Given that C704 is more likely to be associated with behavioral phenotypes,

this could mean that an increased oligomerization of DISC1 C704 could be at the protein equivalent of this genetic polymorphism. How the increased oligomerization is translated in disturbed cellular functions remains unclear: similar to Kamiya et al. (*27*), we could observe only slight differences of DISC1 S/C704 in binding to NDEL1 (Figure 4). This could mean that either (1) these subtle effects are sufficient for eliciting a different biological effect or (2) executive systems other than NDEL1 transmit a DISC1-oligomerization-sensitive signal. Since DISC1 is thought to be part of a quatenary protein complex involving NDEL1, NDE1, LIS1, PDE4B (*42*), and possibly other proteins, the disturbances initiated by DISC1 misassembly may be manifold.

The existence of C-terminal proteolytic DISC1 fragments *in vivo* (Figure 5) potentially adds another level of functional regulation of DISC1. Transgenic expression of an isolated C-terminal domain of DISC1 (671−852) in a mouse model produced a complex schizophrenia-related phenotype, including anatomical abnormalities (*43*). This study suggested that a C-terminal fragment could have a dominant negative effect on physiological DISC1 function, particularly during cerebral development. When we expressed the C-terminal fragment in human cells and analyzed DISC1 complexes by glycerol gradients, we observed DISC1 immunoreactivity over a wide range of fractions, indicating that it had associated to either multimeric complexes, other proteins, or both (Figure 4C). In fact, NDEL1 immunoreactivity shifted to denser fractions, indicating that DISC1multimeric complexes bound NDEL1, thereby building heavier quatenary complexes. However, similar to full-length DISC1, C-terminal DISC1 became also partially insoluble when transiently overexpressed (Figure 4B). These results demonstrate that DISC1 C-terminal fragments can associate to functional assemblies *in vivo*. Whether endogenous C-terminal DISC1 fragments in the CNS can play such a potentially dominant negative role on full-length DISC1 *in vivo* remains to be shown.

ACKNOWLEDGMENT

Post-mortem brain tissue was donated by The Stanley Medical Research Institute's brain collection courtesy of Drs. Michael B. Knable, E. Fuller Torrey, Maree J. Webster, and Robert H. Yolken.

SUPPORTING INFORMATION AVAILABLE

Seven figures with extended in-depth biochemical and biophysical characterization of C-terminal DISC1 constructs. This material is available free of charge via the Internet at http://pubs.acs.org.

REFERENCES

1. Ross, C. A., Margolis, R. L., Reading, S. A., Pletnikov, M., and Coyle, J. T. (2006) Neurobiology of schizophrenia. *Neuron 52*, 139–153.
2. Chubb, J. E., Bradshaw, N. J., Soares, D. C., Porteous, D. J., and Millar, J. K. (2008) The DISC locus in psychiatric illness. *Mol. Psychiatry 13*, 36–64.
3. St. Clair, D., Blackwood, D., Muir, W., Carothers, A., Walker, M., Spowart, G., Gosden, C., and Evans, H. J. (1990) Association within a family of a balanced autosomal translocation with major mental illness. *Lancet 336*, 13–16.
4. Millar, J. K., Wilson-Annan, J. C., Anderson, S., Christie, S., Taylor, M. S., Semple, C. A., Devon, R. S., Clair, D. M., Muir, W. J., Blackwood, D. H., and Porteous, D. J. (2000) Disruption of two novel genes by a translocation co-segregating with schizophrenia. *Hum. Mol. Genet. 9*, 1415–1423.
5. Blackwood, D. H., Fordyce, A., Walker, M. T., St. Clair, D. M., Porteous, D. J., and Muir, W. J. (2001) Schizophrenia and affective disorders—cosegregation with a translocation at chromosome 1q42 that directly disrupts brain-expressed genes: clinical and P300 findings in a family. *Am. J. Hum. Genet. 69*, 428–433.
6. Kamiya, A., Kubo, K., Tomoda, T., Takaki, M., Youn, R., Ozeki, Y., Sawamura, N., Park, U., Kudo, C., Okawa, M., Ross, C. A., Hatten, M. E., Nakajima, K., and Sawa, A. (2005) A schizophrenia-associated mutation of DISC1 perturbs cerebral cortex development. *Nat. Cell Biol. 7*, 1167–1178.
7. Hikida, T., Jaaro-Peled, H., Seshadri, S., Oishi, K., Hookway, C., Kong, S., Wu, D., Xue, R., Andrade, M., Tankou, S., Mori, S., Gallagher, M., Ishizuka, K., Pletnikov, M., Kida, S., and Sawa, A. (2007) Dominant-negative DISC1 transgenic mice display schizophrenia-associated phenotypes detected by measures translatable to humans. *Proc. Natl. Acad. Sci. U.S.A. 104*, 14501–14506.
8. Pletnikov, M. V., Ayhan, Y., Nikolskaia, O., Xu, Y., Ovanesov, M. V., Huang, H., Mori, S., Moran, T. H., and Ross, C. A. (2008) Inducible expression of mutant human DISC1 in mice is associated with brain and behavioral abnormalities reminiscent of schizophrenia. *Mol. Psychiatry 13*, 173–186.
9. Shen, S., Lang, B., Nakamoto, C., Zhang, F., Pu, J., Kuan, S. L., Chatzi, C., He, S., Mackie, I., Brandon, N. J., Marquis, K. L., Day, M., Hurko, O., McCaig, C. D., Riedel, G., and St. Clair, D. (2008) Schizophrenia-related neural and behavioral phenotypes in transgenic mice expressing truncated Disc1. *J. Neurosci. 28*, 10893–10904.
10. Millar, J. K., Pickard, B. S., Mackie, S., James, R., Christie, S., Buchanan, S. R., Malloy, M. P., Chubb, J. E., Huston, E., Baillie, G. S., Thomson, P. A., Hill, E. V., Brandon, N. J., Rain, J. C., Camargo, L. M., Whiting, P. J., Houslay, M. D., Blackwood, D. H., Muir, W. J., and Porteous, D. J. (2005) DISC1 and PDE4B are interacting genetic factors in schizophrenia that regulate cAMP signaling. *Science 310*, 1187–1191.
11. Ekelund, J., Hovatta, I., Parker, A., Paunio, T., Varilo, T., Martin, R., Suhonen, J., Ellonen, P., Chan, G., Sinsheimer, J. S., Sobel, E., Juvonen, H., Arajarvi, R., Partonen, T., Suvisaari, J., Lonnqvist, J., Meyer, J., and Peltonen, L. (2001) Chromosome 1 loci in Finnish schizophrenia families. *Hum. Mol. Genet. 10*, 1611–1617.
12. Hamshere, M. L., Bennett, P., Williams, N., Segurado, R., Cardno, A., Norton, N., Lambert, D., Williams, H., Kirov, G., Corvin, A., Holmans, P., Jones, L., Jones, I., Gill, M., O'Donovan, M. C., Owen, M. J., and Craddock, N. (2005) Genomewide linkage scan in schizoaffective disorder: significant evidence for linkage at 1q42 close to DISC1, and suggestive evidence at 22q11 and 19p13. *Arch. Gen. Psychiatry 62*, 1081–1088.
13. Hwu, H. G., Liu, C. M., Fann, C. S., Ou-Yang, W. C., and Lee, S. F. (2003) Linkage of schizophrenia with chromosome 1q loci in Taiwanese families. *Mol. Psychiatry 8*, 445–452.
14. Callicott, J. H., Straub, R. E., Pezawas, L., Egan, M. F., Mattay, V. S., Hariri, A. R., Verchinski, B. A., Meyer-Lindenberg, A., Balkissoon, R., Kolachana, B., Goldberg, T. E., and Weinberger, D. R. (2005) Variation in DISC1 affects hippocampal structure and function and increases risk for schizophrenia. *Proc. Natl. Acad. Sci. U.S.A. 102*, 8627–8632.
15. Hashimoto, R., Numakawa, T., Ohnishi, T., Kumamaru, E., Yagasaki, Y., Ishimoto, T., Mori, T., Nemoto, K., Adachi, N., Izumi, A., Chiba, S., Noguchi, H., Suzuki, T., Iwata, N., Ozaki, N., Taguchi, T., Kamiya, A., Kosuga, A., Tatsumi, M., Kamijima, K., Weinberger, D. R., Sawa, A., and Kunugi, H. (2006) Impact of the DISC1 Ser704Cys polymorphism on risk for major depression, brain morphology and ERK signaling. *Hum. Mol. Genet. 15*, 3024–3033.
16. Qu, M., Tang, F., Yue, W., Ruan, Y., Lu, T., Liu, Z., Zhang, H., Han, Y., Zhang, D., Wang, F., and Zhang, D. (2007) Positive association of the Disrupted-in-Schizophrenia-1 gene (DISC1) with schizophrenia in the Chinese Han population. *Am. J. Med. Genet. 144B*, 266–270.
17. Thomson, P. A., Harris, S. E., Starr, J. M., Whalley, L. J., Porteous, D. J., and Deary, I. J. (2005) Association between genotype at an exonic SNP in DISC1 and normal cognitive aging. *Neurosci. Lett. 389*, 41–45.
18. Morris, J. A., Kandpal, G., Ma, L., and Austin, C. P. (2003) DISC1 (Disrupted-In-Schizophrenia 1) is a centrosome-associated protein that interacts with MAP1A, MIPT3, ATF4/5 and NUDEL: regulation and loss of interaction with mutation. *Hum. Mol. Genet. 12*, 1591–1608.
19. James, R., Adams, R. R., Christie, S., Buchanan, S. R., Porteous, D. J., and Millar, J. K. (2004) Disrupted in Schizophrenia 1 (DISC1) is a multicompartmentalized protein that predominantly localizes to mitochondria. *Mol. Cell. Neurosci. 26*, 112–122.

20. Millar, J. K., James, R., Christie, S., and Porteous, D. J. (2005) Disrupted in schizophrenia 1 (DISC1): subcellular targeting and induction of ring mitochondria. *Mol. Cell. Neurosci. 30*, 477–484.
21. Ishizuka, K., Paek, M., Kamiya, A., and Sawa, A. (2006) A review of Disrupted-In-Schizophrenia-1 (DISC1): neurodevelopment, cognition, and mental conditions. *Biol. Psychiatry 59*, 1189–1197.
22. Ozeki, Y., Tomoda, T., Kleiderlein, J., Kamiya, A., Bord, L., Fujii, K., Okawa, M., Yamada, N., Hatten, M. E., Snyder, S. H., Ross, C. A., and Sawa, A. (2003) Disrupted-in-Schizophrenia-1 (DISC-1): mutant truncation prevents binding to NudE-like (NUDEL) and inhibits neurite outgrowth. *Proc. Natl. Acad. Sci. U.S.A. 100*, 289–294.
23. Mao, Y., Ge, X., Frank, C. L., Madison, J. M., Koehler, A. N., Doud, M. K., Tassa, C., Berry, E. M., Soda, T., Singh, K. K., Biechele, T., Petryshen, T. L., Moon, R. T., Haggarty, S. J., and Tsai, L. H. (2009) Disrupted in schizophrenia 1 regulates neuronal progenitor proliferation via modulation of GSK3beta/beta-catenin signaling. *Cell 136*, 1017–1031.
24. Brandon, N. J., Handford, E. J., Schurov, I., Rain, J. C., Pelling, M., Duran-Jimeniz, B., Camargo, L. M., Oliver, K. R., Beher, D., Shearman, M. S., and Whiting, P. J. (2004) Disrupted in Schizophrenia 1 and Nudel form a neurodevelopmentally regulated protein complex: implications for schizophrenia and other major neurological disorders. *Mol. Cell. Neurosci. 25*, 42–55.
25. Brandon, N. J. (2007) Dissecting DISC1 function through protein-protein interactions. *Biochem. Soc. Trans. 35*, 1283–1286.
26. Camargo, L. M., Collura, V., Rain, J. C., Mizuguchi, K., Hermjakob, H., Kerrien, S., Bonnert, T. P., Whiting, P. J., and Brandon, N. J. (2007) Disrupted in Schizophrenia 1 Interactome: evidence for the close connectivity of risk genes and a potential synaptic basis for schizophrenia. *Mol. Psychiatry 12*, 74–86.
27. Kamiya, A., Tomoda, T., Chang, J., Takaki, M., Zhan, C., Morita, M., Cascio, M. B., Elashvili, S., Koizumi, H., Takanezawa, Y., Dickerson, F., Yolken, R., Arai, H., and Sawa, A. (2006) DISC1-NDEL1/NUDEL protein interaction, an essential component for neurite outgrowth, is modulated by genetic variations of DISC1. *Hum. Mol. Genet. 15*, 3313–3323.
28. Leliveld, S., Bader, V., Hendriks, P., Prikulis, I., Sajnani, G., Requena, J. R., and Korth, C. (2008) Insolubility of DISC1 disrupts oligomer-dependent interactions with NDEL1 and is associated with sporadic mental disease. *J. Neurosci. 28*, 3839–3845.
29. Cuff, J. A., Clamp, M. E., Siddiqui, A. S., Finlay, M., and Barton, G. J. (1998) JPred: a consensus secondary structure prediction server. *Bioinformatics 14*, 892–893.
30. McGuffin, L. J., Bryson, K., and Jones, D. T. (2000) The PSIPRED protein structure prediction server. *Bioinformatics 16*, 404–405.
31. Rost, B. (1996) PHD: predicting one-dimensional protein structure by profile-based neural networks. *Methods Enzymol. 266*, 525–539.
32. Gruber, M., Soding, J., and Lupas, A. N. (2006) Comparative analysis of coiled-coil prediction methods. *J. Struct. Biol. 155*, 140–145.
33. Mason, J. M., and Arndt, K. M. (2004) Coiled coil domains: stability, specificity, and biological implications. *ChemBioChem 5*, 170–176.
34. Torrey, E. F., Webster, M., Knable, M., Johnston, N., and Yolken, R. H. (2000) The Stanley Foundation brain collection and neuropathology consortium. *Schizophr. Res. 44*, 151–155.
35. Lobley, A., Whitmore, L., and Wallace, B. A. (2002) DICHROWEB: an interactive website for the analysis of protein secondary structure from circular dichroism spectra. *Bioinformatics 18*, 211–212.
36. Franzen, B., Yang, Y., Sunnemark, D., Wickman, M., Ottervald, J., Oppermann, M., and Sandberg, K. (2003) Dihydropyrimidinase related protein-2 as a biomarker for temperature and time dependent post mortem changes in the mouse brain proteome. *Proteomics 3*, 1920–1929.
37. Korth, C., Stierli, B., Streit, P., Moser, M., Schaller, O., Fischer, R., Schulz-Schaeffer, W., Kretzschmar, H., Raeber, A., Braun, U., Ehrensperger, F., Hornemann, S., Glockshuber, R., Riek, R., Billeter, M., Wuthrick, K., and Oesch, B. (1997) Prion (PrP^{Sc})-specific epitope defined by a monoclonal antibody. *Nature 389*, 74–77.
38. Taylor, M. S., Devon, R. S., Millar, J. K., and Porteous, D. J. (2003) Evolutionary constraints on the Disrupted in Schizophrenia locus. *Genomics 81*, 67–77.
39. Prusiner, S. B. (2001) Shattuck Lecture—Neurodegenerative diseases and prions. *N. Engl. J. Med. 344*, 1516–1526.
40. Taylor, J. P., Hardy, J., and Fischbeck, K. H. (2002) Toxic proteins in neurodegenerative disease. *Science 296*, 1991–1995.
41. Di Giorgio, A., Blasi, G., Sambataro, F., Rampino, A., Papazacharias, A., Gambi, F., Romano, R., Caforio, G., Rizzo, M., Latorre, V., Popolizio, T., Kolachana, B., Callicott, J. H., Nardini, M., Weinberger, D. R., and Bertolino, A. (2008) Association of the SerCys DISC1 polymorphism with human hippocampal formation gray matter and function during memory encoding. *Eur. J. Neurosci. 28*, 2129–2136.
42. Bradshaw, N. J., Ogawa, F., Antolin-Fontes, B., Chubb, J. E., Carlyle, B. C., Christie, S., Claessens, A., Porteous, D. J., and Millar, J. K. (2008) DISC1, PDE4B, and NDE1 at the centrosome and synapse. *Biochem. Biophys. Res. Commun. 377*, 1091–1096.
43. Li, W., Zhou, Y., Jentsch, J. D., Brown, R. A., Tian, X., Ehninger, D., Hennah, W., Peltonen, L., Lonnqvist, J., Huttunen, M. O., Kaprio, J., Trachtenberg, J. T., Silva, A. J., and Cannon, T. D. (2007) Specific developmental disruption of disrupted-in-schizophrenia-1 function results in schizophrenia-related phenotypes in mice. *Proc. Natl. Acad. Sci. U.S.A. 104*, 18280–18285.
44. Lupas, A., Van Dyke, M., and Stock, J. (1991) Predicting coiled coils from protein sequences. *Science 252*, 1162–1164.
45. Berger, B., Wilson, D. B., Wolf, E., Tonchev, T., Milla, M., and Kim, P. S. (1995) Predicting coiled coils by use of pairwise residue correlations. *Proc. Natl. Acad. Sci. U.S.A. 92*, 8259–8263.
46. Delorenzi, M., and Speed, T. (2002) An HMM model for coiled-coil domains and a comparison with PSSM-based predictions. *Bioinformatics 18*, 617–625.